PLOS | ONE

RESEARCH ARTICLE

Targeted Cancer Therapy with a Novel Anti-CD37 Beta-Particle Emitting Radioimmunoconjugate for Treatment of Non-Hodgkin Lymphoma

Ada H. V. Repetto-Llamazares[1,2]*, Roy H. Larsen[3], Sebastian Patzke[2], Karianne G. Fleten[4], David Didierlaurent[5], Alexandre Pichard[6], Jean Pierre Pouget[6], Jostein Dahle[1]

1 Nordic Nanovector ASA, Kjelsåsveien 168, 0884, Oslo, Norway, **2** Department of Radiation Biology, Institute for Cancer Research, Oslo University Hospital, Montebello, 0310, Oslo, Norway, **3** Sciencons AS, Kjelsåsveien 168, 0884, Oslo, Norway, **4** Department of Tumor Biology, Institute for Cancer Research, Oslo University Hospital, Montebello, 0310, Oslo, Norway, **5** UMR 1037 INSERM/UPS, Centre de Recherche en Cancérologie de Toulouse, Toulouse, F-31062, France, **6** Institut de Recherche en Cancérologie de Montpellier, Institut National de la Santé et de la Recherche Médicale, U896, Université Montpellier, Montpellier, France

* arepetto@nordicnanovector.com

OPEN ACCESS

Citation: Repetto-Llamazares AHV, Larsen RH, Patzke S, Fleten KG, Didierlaurent D, Pichard A, et al. (2015) Targeted Cancer Therapy with a Novel Anti-CD37 Beta-Particle Emitting Radioimmunoconjugate for Treatment of Non-Hodgkin Lymphoma. PLoS ONE 10(6): e0128816. doi:10.1371/journal.pone.0128816

Academic Editor: Ken Mills, Queen's University Belfast, UNITED KINGDOM

Received: February 9, 2015

Accepted: April 30, 2015

Published: June 11, 2015

Data Availability Statement: All relevant data are within the paper and its Supporting Information files.

Funding: This study was partially funded by the Norwegian Research Council (http://www.forskningsradet.no) grant numbers 213633 and 219454 and by Nordic Nanovector ASA (http://www.nordicnanovector.com). Co-authors Ada H. V. Repetto-Llamazares and Jostein Dahle are employed by Nordic Nanovector ASA. Nordic Nanovector ASA provided support in the form of salaries for authors AHVR-L and JD, but did not have any additional role

Abstract

^{177}Lu-DOTA-HH1 (^{177}Lu-HH1) is a novel anti-CD37 radioimmunoconjugate developed to treat non-Hodgkin lymphoma. Mice with subcutaneous Ramos xenografts were treated with different activities of ^{177}Lu-HH1, ^{177}Lu-DOTA-rituximab (^{177}Lu-rituximab) and non-specific ^{177}Lu-DOTA-IgG$_1$ (^{177}Lu-IgG$_1$) and therapeutic effect and toxicity of the treatment were monitored. Significant tumor growth delay and increased survival of mice were observed in mice treated with 530 MBq/kg ^{177}Lu-HH1 as compared with mice treated with similar activities of ^{177}Lu-rituximab or non-specific ^{177}Lu-IgG1, 0.9% NaCl or unlabeled HH1. All mice injected with 530 MBq/kg of ^{177}Lu-HH1 tolerated the treatment well. In contrast, 6 out of 10 mice treated with 530 MBq/kg ^{177}Lu-rituximab experienced severe radiation toxicity. The retention of ^{177}Lu-rituximab in organs of the mononuclear phagocyte system was longer than for ^{177}Lu-HH1, which explains the higher toxicity observed in mice treated with ^{177}Lu-rituximab. *In vitro* internalization studies showed that ^{177}Lu-HH1 internalizes faster and to a higher extent than ^{177}Lu-rituximab which might be the reason for the better therapeutic effect of ^{177}Lu-HH1.

Introduction

Despite the promise of therapy using the naked monoclonal antibody (mAb) rituximab, a substantial number of the patients treated with conventional doses of rituximab alone or in combination with chemotherapy do not obtain complete response and may eventually relapse [1]. Alternative treatments have been anti-CD20 mAbs conjugated to ^{131}I (tositumomab) or ^{90}Y

in the study design, data collection and analysis, decision to publish, or preparation of the manuscript. Co-author Roy H. Larsen is affiliated to Sciencons AS. Sciencons AS is a shareholder of Nordic Nanovector ASA. Sciencons AS did not provide support in the form of salary for author RHL, and did not have any additional role in the study design, data collection and analysis, decision to publish, or preparation of the manuscript. The specific roles of these authors are articulated in the 'author contributions' section.

Competing Interests: This study was funded in part by Nordic Nanovector ASA (http://www.nordicnanovector.com/). The authors Jostein Dahle and Ada H. V. Repetto-Llamazares are employed by Nordic Nanovector ASA, and Roy H. Larsen is a member of the Board of Nordic Nanovector ASA and Sciencons AS and the three of them are shareholders of Nordic Nanovector ASA. 177Lu-HH1 is the main product from Nordic Nanovector ASA. There are no patents, further products in development or further marketed products to declare. This does not alter the authors' adherence to all the PLoS ONE policies on sharing data and materials

(ibritumomab-tiuxetan). Treatment with conventional activities of the radiolabeled mAbs has produced higher overall response and complete remission rates compared with naked mAbs [2–5]. Considering that radioimmunotherapy (RIT) is mostly used after patients have been treated with several rounds of rituximab and that the two approved radioimmunoconjugates (RICs) for clinical use, ^{90}Y-ibritumomab-tiuxetan (Zevalin) and ^{131}I-tositumomab (Bexxar), target the same CD20 antigen as rituximab, it is desirable to design a new RIC that will target a different antigen than CD20. The CD37 antigen is abundantly expressed in B-cells, but is absent on plasma cells and normal stem cells [6–8]. Therefore, CD37 seems to be an appropriate therapeutic target in patients with relapsed B-cell derived malignancies, such as B-cell CLL, hairy-cell leukemia (HCL) and B-cell NHL.

RIT with CD37 as target has previously been explored using a ^{131}I-labeled murine monoclonal antibody (MB-1) both in a mouse model and in patients [9–14]. A higher degree of internalization and degradation of ^{131}I-labeled RIC was found for CD37 than for CD20 [14]. Despite promising clinical responses observed in these clinical studies for the anti-CD37 antibody, further development of RIT focused on CD20 as the target antigen and no subsequent efforts have been made to develop RIT with anti-CD37-based RICs. A limited number of other CD37-directed antibody based immunotherapies have, however, been evaluated in patients. The small modular immunopharmaceutical protein Otlertuzumab has advanced into clinical testing [15] and recently reported on phase II data in combination with bendamustine [16]. In addition, the Fc-engineered antibody CD37.1 (BI836826) [17] has recently entered phase I [18]. Furthermore, two antibody-drug conjugates (ADCs) have been developed that covalently link cytotoxic agents to CD37-targeting antibodies to enhance their antitumor potency: IMGN529 [19] and AGS-67E [20]. ADCs are designed to give specific delivery of cytotoxic compounds to cells expressing the target antigen, through ADC binding, internalization, and intracellular payload release. Clinical data have demonstrated the potential of ADCs for cancer therapy of CD30 and HER2 positive tumors [21,22]. All these CD37 targeting drugs had shown promising results, which further validates CD37 as a target for treatment of NHL and CLL. An advantage with RIT compared with naked mAbs and ADCs is the range of the emitted radiation, which gives a cross-fire effect so that tumor cells with less antigens or non-accessible tumor cells also get hit by the cytotoxic radiation. It remains to be seen if the mechanism of action of RIT is better than that of ADCs.

The potency of RIT against the internalizing antigen CD37 might have been underestimated by the use of the radionuclide ^{131}I, which tends to be cleaved off from the antibody and excreted from the cells upon internalization and catabolism when used as "non-residualizing" tyrosine-incorporated radiolabel, as was done in the early studies with ^{131}I-MB-1 [23]. "Residualizing" radiolabels, on the other hand, are trapped in the cells after metabolism of the RIC. In an effort to re-evaluate and improve RIT against CD37 we have developed a new RIC (Betalutin) based on the "residualizing" radiolabel ^{177}Lu linked to the anti-CD37 antibody HH1 [24]. Treatment with 100 MBq/kg ^{177}Lu-HH1 resulted in a threefold increase in the survival of SCID mice that were intravenously injected with Daudi lymphoma cells compared to untreated control mice [7]. SCID mice are not able to repair DNA double strand breaks [25], limiting the amount of radioactivity that can be administered, while nude mice can tolerate higher doses of radiation. A subcutaneous tumor xenograft in nude mice is a more relevant model for the bulky type of disease that is often found in NHL patients than the intravenous model in SCID mice. Therefore, the therapeutic and toxicity effect of ^{177}Lu-HH1 was evaluated in nude mice with subcutaneous Ramos xenografts in the present paper.

Materials and Methods

Tumor cells

Ramos lymphoma cells (LGC Standards, Boras, Sweden) expressing the CD20 and CD37 receptors were grown in RPMI 1640 medium supplemented with Glutamax (Gibco, Paisley, UK), 10% heat-inactivated FCS (Gibco) and 1% penicillin-streptomycin (Gibco) in a humid atmosphere with 95% air/5% CO_2.

Radiolabeling of antibodies

The antibodies HH1 (anti-CD37, Nordic Nanovector ASA, Oslo, Norway), Rituximab (anti-CD20, Roche, Pharma Schweiz, Basel, Switzerland) and the murine non-specific isotype control antibody (IgG_1) (MAB002, R&D Systems Inc., Minneapolis, USA) were labeled with the chelator p-SCN-Bn-DOTA (DOTA, Macrocyclics, TX, USA) and subsequently labeled with ^{177}Lu (ITG, Garching, Germany) as previously described [26]. Labeling with ^{125}I (Hartmann Analytic, Braunschweig, Germany) was performed using iodogen tubes (Pierce, Rockford, IL, USA) as described previously [23].

The immunoreactivity (IRF) of all the tumor specific RICs was verified using a modified Lindmo method [27] with one cell concentration of 75 million cells/ml. The IRF of all specific RICs was between 57% and 76%.

Number of cell surface receptors

Scatchard analyses were performed using ^{177}Lu-HH1 or ^{125}I-rituximab. A concentration of 10 million cells/ml of Ramos lymphoma cells were incubated for 1 hour with increasing amounts of radioimmunoconjugates (between 0 and 6.25 nM). Cells previously blocked with unlabeled antibody were used to account for non-specific binding. Each sample was measured in duplicates and the results were averaged. After incubation with the RIC, the activity in each sample was measured using a gamma counter (Cobra gamma; Packard Instrument Co, Meriden, CT, USA) and cells were washed two times using DPBS (Gibco, Paisley, UK) supplemented with 0.5%wt Bovine Serum Albumin (BDH Prolabo, VWR, Lutterworth, Leicestershire, UK), after which the activity bound to the cells was counted in the gamma counter. The equilibrium dissociation constant (K_d) and maximum average density of antigens (B_{max}) was calculated from the fitting of the experimental data. Three experiments were performed using ^{177}Lu-HH1 and 2 experiments using ^{125}I-rituximab. The results from all experiments for each RIC were averaged to obtain an average value of K_d and B_{max} for each RIC.

Internalization experiments

HH1-DOTA was labeled with Alexa Fluor 488 and rituximab with Alexa Fluor 647 (Molecular Probes, Invitrogen, Paisley, UK). One million Ramos cells per ml in growth medium were incubated with 10 μg/ml of HH1 or 20 μg/ml of rituximab for either 19 hours at 37°C or 1 h at around 4°C. Hoechst 33342 (Sigma-Aldrich, St.Louis, MO, US) was added to the cells to a concentration of 2 μg/ml 1 hour before imaging. Cells were imaged with an AxioImager Z1 ApoTome microscope system (Carl Zeiss, Jena, DE) using a PlanApo 63×/N.A.1.4 DIC lens, appropriate optical filters, an AxioCam MRm camera and Axiovision 4.8.2 (Carl Zeiss). Z-sections were obtained for every 1 μm across the entire cell volume. Images are presented as overlays of fluorescence images of central z-section and DIC image. 20 to 40 cells were scanned for each treatment.

Table 1. Overview of therapy and toxicity experiments in nude mice with Ramos xenografts.

Experiment	Treatments	mice/ group	Mice age[a] (weeks)	Mice weights[b] (g)	Tumor volumes[b], (mm^3)
1	530 MBq/kg ^{177}Lu-HH1, 530 MBq/kg ^{177}Lu-rituximab, 530 MBq/kg ^{177}Lu-IgG1, 15 μg/kg HH1, 0.9% NaCl	9–10	6–8	21.1–29.0 (25 ± 2)	20–780 (139 ± 134)
2	410 MBq/kg ^{177}Lu-HH1, 300 MBq/kg ^{177}Lu-rituximab, 0.9% NaCl.	5–6	6–8	21.0–29.7 (25 ± 2)	22–760 (342 ± 221)

[a]At implantation of xenografts.

[b]At treatment injection Min-Max (Average ± SD).

doi:10.1371/journal.pone.0128816.t001

Animals and xenografts

Institutionally bred female Athymic nude FOX1^{nu} mice were used. Age and weight of the mice are given in Table 1. The animals were maintained under pathogen-free conditions with a 12 hours lighting cycle at a room temperature of 23°C and air relative humidity of 55% in plastic cages. Food and water were supplied *ad libitum* and bedding was changed regularly. Mice were anesthetized with subcutaneous injections of 70–100 μl Tiletamin-Zolazepam mix (Virbac, Carros Cedex, France) diluted 1:5 with sterile water before implantation of pieces of Ramos lymphoma xenograft tissue from carrier mice, (diameter 1.5–2 mm) in the flanks. All procedures and experiments involving animals in this study were approved by The Norwegian Animal Research Authority (NARA). The Department of Comparative Medicine institutional veterinarian has established the rules for feeding, monitoring, handling, and sacrifice of animals in compliance with regulations set by the Ministry of Agriculture of Norway and "The European Convention for the Protection of Vertebrate Animals used for Experimental and other Scientific Purposes". The institutional veterinarian has delegated authority from the Norwegian Animal Research Authority (NARA). The laboratory animal facilities are subject to a routine health-monitoring program and tested for infectious organisms according to a modification of Federation of European Laboratory Animal Science Associations (FELASA) recommendations.

Therapy and toxicity experiments

Animals bearing growing tumors with diameters between 4 and 12 mm were randomized in cages according to treatment group and were administered intravenously with 100 μl of injection solutions adjusted for individual mouse weight. Two preliminary experiments were performed with injection of activities between 50 and 1000 MBq/kg ^{177}Lu-HH1 (S1 File). These experiments were used to decide the experimental parameters chosen for the two experiments presented in this paper (Table 1) which included injected activities of 410 and 530 MBq/kg ^{177}Lu-HH1, 300 and 530 MBq/kg ^{177}Lu-rituximab, 530 MBq/kg ^{177}Lu-IgG$_1$ and 15 μg/kg HH1 and 0.9% NaCl as control groups.

The mice were weighed and clinically observed two to three times a week for up to 109 days. In addition the mice were monitored daily for any sign of illness or discomfort. Activity level, skin condition (eczema, hemorrhages, etc.) and general health of the mice were observed daily. Mice were euthanized by cervical dislocation under Sevoflurane gas anesthesia if any of the following humane end points were reached: tumor diameter exceeded 20 mm, body weight decreased by 20% from highest body weight or animals otherwise showed symptoms of severe illness and discomfort.

Tumor growth was monitored up to the first tumor volume measurement higher than 2000 mm^3 in each mouse (bigger tumors usually develop necrotic wounds). Complete remission was

defined as no observable tumor. Mice reaching this stage were considered as long term responders.

Hematology. Blood samples were taken prior to injection, at death and every 4 to 7 weeks after treatment administration. The blood sampling was performed as described previously [26]. Radiation toxicity was defined as white blood cell counts below 1×10^9 1/L, platelet counts below 400×10^9 1/L, sudden weight loss—around 5% in the lapse of 2 to 3 day- accompanied by a low activity level, and a general state of sickness. Comparisons between average values of different treatment groups were done using t-tests with a significance level of 0.05.

One mouse treated with 530 MBq/kg ^{177}Lu-HH1 was sacrificed 11 days after treatment injection in order to obtain hematology and histology data at this particular time point. Furthermore, to obtain more hematological data 3 mice having tumor diameters between 12 and 15 mm (800 and 1300 mm3) were also included in experiment 2.

Histopathology. Mice were necropsied and heart, lungs, liver, stomach, spleen, small and large intestines, kidneys, femur, muscle, skull, brain, tumor, skin, ovaries and lymph nodes were fixed and shipped to Accelera, Milano, Italy for casting, sectioning, staining and pathological examination.

Biodistribution experiments

Conjugates were administered by tail vein injection of 100 μl solution (0.2 and 0.9 MBq) to each animal. Between 4 and 7 mice were sacrificed by neck dislocation under Sevoflurane gas anesthesia at each time point after cardiac puncture for blood sampling. Tumor sizes at injection of conjugates varied between 120 and 1800 mm^3. Studies were conducted as described in reference [28]. Comparisons between average values were done using t-tests with a significance level of 0.05.

A pilot *In vivo* SPECT/CT was performed on 2 mice with Ramos subcutaneous xenografts with diameters around 12 mm in their right flank in a nanoSPECT/CT (Bioscan Inc., Washington DC, USA). SPECT/CT acquisitions were performed at 3, 24 and 48 hours after treatment injection in mouse 1 and after 24 hours in mouse 2. Activities measured by SPECT/CT were compared with ex-vivo measurements done at 48 hours after treatment administration. Mice were injected i.v. with 150 μl of 10 MBq of ^{177}Lu-HH1 and were anaesthetized with 2% Isofluran for image acquisition.

Dosimetry

The dose rate and absorbed doses from ^{177}Lu-HH1 and ^{177}Lu-rituximab in mice were calculated as described in reference [28] for an injection of 1 MBq/mouse (40 MBq/kg) and assuming the mean energy of the β-particles, Auger- and conversion electrons to be 0.1473 MeV [29]. The self-radiation fraction for tumor was estimated to be 0.944 (200 mg tumor [30]).

Statistical analysis

The survival of the different treatment groups was compared by Kaplan-Meyer survival analysis using SigmaPlot for Windows version 12.0 (Systat Software Inc., California, USA) using time to reach a tumor volume higher than 4 times the initial tumor volume or euthanasia due to radiation toxicity symptoms as the end points. Hematology and biodistribution data were compared using one-way ANOVA. Multiple comparisons were performed using the Holm Sidak method. A significance level of $p < 0.05$ was used in all tests.

Results

Therapy and toxicity experiments

Tumor growth and survival. There was a marked tumor growth delay in mice treated with 530 MBq/kg ^{177}Lu-HH1 when compared to mice treated with either ^{177}Lu-IgG$_1$ or 0.9% NaCl (Fig 1A). Tumor growth was also delayed in some of the mice treated with 530 MBq/kg ^{177}Lu-rituximab, but this treatment proved to be toxic: 60% of the mice had to be sacrificed due to symptoms of severe radiation toxicity between 11 and 18 days after injection of treatment (Table 2). None of the mice were sacrificed due to radiation toxicity symptoms in any of the other treatment groups. Tumor growth in the control mice treated with 0.9% NaCl or 15 μg/kg naked HH1 was non-homogeneous, with 30% and 10% complete remission, respectively. On the other hand, tumors in mice treated with 530 MBq/kg ^{177}Lu-IgG$_1$ grew homogeneously and did not show any natural regressions. The number of long term responders was highest in mice treated with 530 MBq/kg ^{177}Lu-HH1 (Fig 1B). Furthermore, treatment with 530 MBq/kg ^{177}Lu-HH1 significantly extended the survival of mice compared with ^{177}Lu-IgG$_1$, 0.9% NaCl and HH1 ($p < 0.05$) (Fig 1C, Table 2). Survival of mice treated with ^{177}Lu-IgG$_1$ was significantly shorter than for those treated with 0.9% NaCl ($p < 0.05$), which was due to the growth homogeneity and the lack of tumor regression observed in mice treated with ^{177}Lu-IgG$_1$, which might be related to radiation induced immunosuppression. It has been previously shown that growth of xenografts in mice can be enhanced by whole body irradiation (WBI) [31–34] or other immunomodulating agents [32,35–38]. Natural regressions of xenografts in nude mice in control groups have been observed previously [33,35], especially in nude mice with subcutaneous Ramos xenografts [39,40]. RIT can be regarded as a type of WBI treatment, which may therefore result in better take and growth of xenografts in treated mice than in control mice. Thus, the therapeutic efficacy of RIT might be underestimated in mouse models where total body irradiation enhances tumor growth, especially when comparing the therapeutic effect of RICs with agents having low systemic toxicity such as NaCl or unlabeled mAbs. It might be more convenient, therefore, to compare the effect of RICs to corresponding dosages of non-specific, control RICs instead.

Given the high toxicity observed during the first two weeks in some of the mice treated with ^{177}Lu-rituximab, one more experiment was performed using lower activities. Treatments with 410 MBq/kg ^{177}Lu-HH1 and 300 MBq/kg ^{177}Lu-rituximab (approximately 50% of the LD50 of each RIC) resulted in a slight tumor growth delay (Fig 2A). Mice treated with 410 MBq/kg ^{177}Lu-HH1 had the highest number of long term responders while there was no long term responders in mice treated with 300 MBq/kg ^{177}Lu-rituximab due to no inhibition of tumor growth (Fig 2B). Median survival was longer in mice treated with 410 MBq/kg ^{177}Lu-HH1 (more than 15 times compared to the control group) but the difference was not statistically significant compared with the other treatment groups ($p > 0.05$) (Fig 2C, Table 2). Median survival of mice treated with 300 MBq/kg ^{177}Lu-rituximab was around 3 times longer than for the mice in the control group, while the median survival of mice treated with 530 MBq/kg ^{177}Lu-rituximab was similar to the mice in the control group. Even when the amount of long term responders was higher for the higher injected activity of ^{177}Lu-rituximab the toxicity of the treatment had a strong impact on the median survival. The optimal injected activity for ^{177}Lu-rituximab might lie in between 300 and 530 MBq/kg, where an optimal amount of long term responders could be found without life-threatening toxicity.

Body weight. The average body weight of mice treated with RICs decreased sharply after injection. The average body weight loss lasted for around 7 days for treatment with 530 MBq/kg and around 4 days for treatment with 410 and 300 MBq/kg activities (Fig 3). Afterwards, the

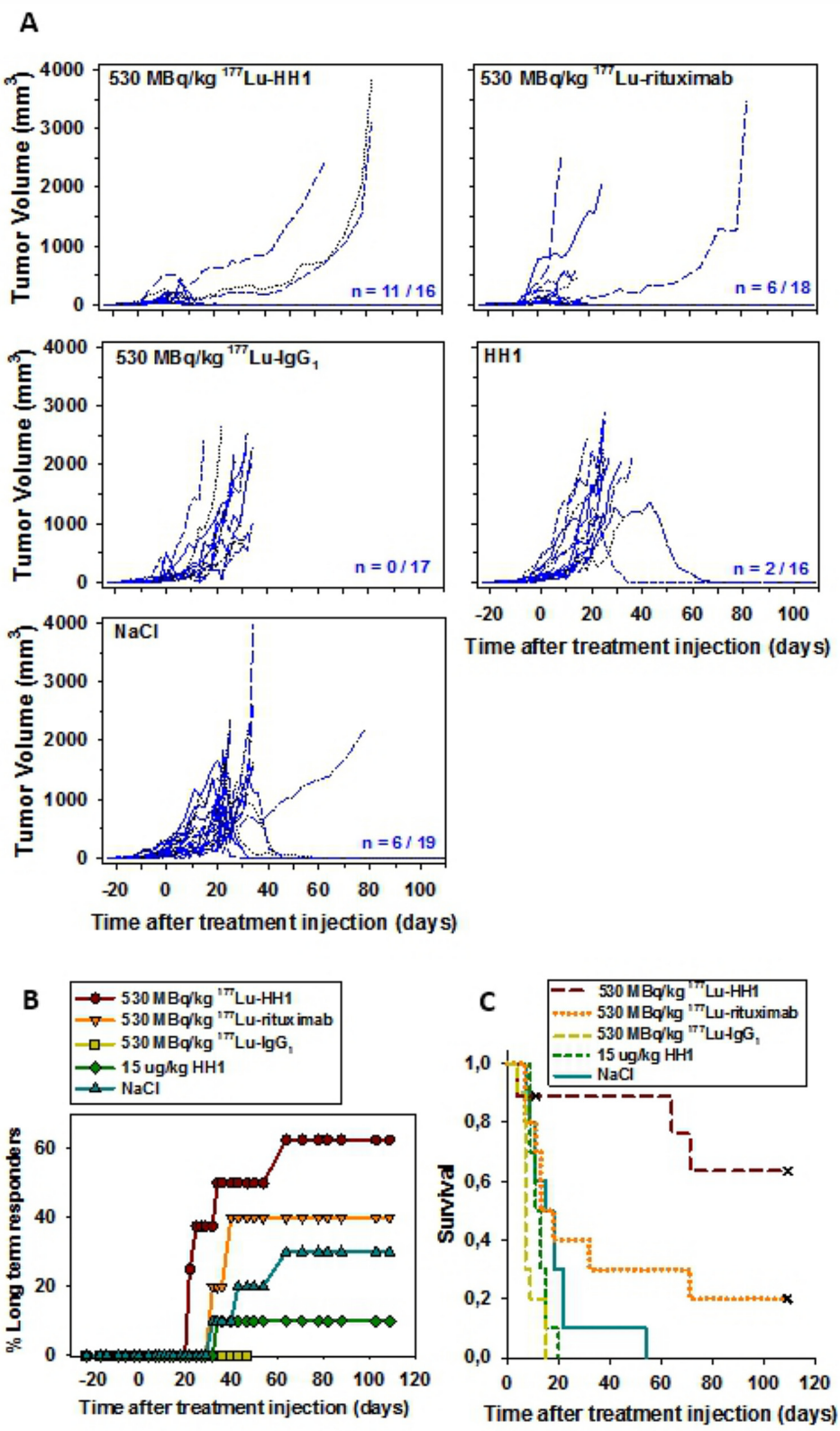

Fig 1. Tumor growth, long term responders and survival of nude mice with Ramos xenografts after treatment with 530 MBq/kg ^{177}Lu-HH1, 530 MBq/kg ^{177}Lu-rituximab, 530 MBq/kg ^{177}Lu-IgG$_1$ non-specific isotype control, 15 μg/kg HH1 and 0.9% NaCl. (A) Individual tumor growth (n = Number of tumors

in remission at the end of study/total number of initial tumors); (B) Percentage of long term responders (mice euthanized due to radiation toxicity symptoms or for hematology measurements before one of their tumors reached a volume of 2000 mm^3 were not considered in the analysis); (C) Kaplan-Meier survival curve. End point: tumor volume $\geq$ 4 times initial tumor volume. Crosses represent censored animals that were euthanized before reaching 4 times the initial tumor volume. N = 9–10. Multiple comparisons were performed using Holm Sidak method. Significance level: $p < 0.05$.

doi:10.1371/journal.pone.0128816.g001

average body weight of the treated mice began to increase, tending toward the average body weight of the control groups.

Hematology. The average numbers of White Blood Cells (WBC) and Red Blood Cells (RBC) for mice treated with 530 MBq/kg of the different RICs were below the values for the NaCl control group for 4 and 8 weeks but normalized at the end of the study (Fig 4A). The average number of platelets (PLT) did not vary significantly between treatment and control groups. However, between 11 and 25 days after treatment with RICs, WBC, RBC and PLT numbers were considerably lower in mice treated with 530 MBq/kg, indicating a nadir around 2 weeks after treatment administration. There were no control animals sacrificed in this time range, but control values can be assumed to be close to those measured at baseline and around 4 weeks after treatment injection in the NaCl group.

The average number of WBC in mice treated with 410 MBq/kg ^{177}Lu-HH1 and 300 MBq/kg ^{177}Lu-rituximab was significantly lower than for the control group 4 weeks after treatment administration, but the values normalized towards the end of the experiment (Fig 4B). The average number of RBC and PLT were similar for all treatment groups ($p > 0.05$). There were no deaths associated to severe symptoms of radiation toxicity in this experiment. However, WBC counts in mice treated with ^{177}Lu-rituximab that were sacrificed at 13 and 17 days due to tumor diameter higher than 20 mm had WBC, RBC and PLT values considerably lower than the values measured for NaCl at similar time points.

Histopathology. The main organs affected by treatment with RICs with activities equal to or higher than 530 MBq/kg were the bone marrow, lymph nodes, spleen and ovaries. Animals treated with 530 MBq/kg ^{177}Lu-rituximab showed severe changes in hemato-lymphopoietic tissues, including decreased extra-medullary hematopoiesis, lymphoid depletion in the spleen and atrophy of the bone marrow (Fig 5A), indicating radiation damage (Table 3). These observations were more severe the sooner the mice had to be sacrificed after treatment injection.

Table 2. Median survival time of mice and percentage of mice euthanized due to radiation toxicity after treatment with 530 MBq/kg ^{177}Lu-HH1, ^{177}Lu-rituxmab and ^{177}Lu-IgG$_1$ non-specific isotype control, HH1 or NaCl.

Experiment	Group	Median survival time ± SE (days)	Radiation Toxicity (%)
1	NaCl	18 ± 3[a]	0
	HH1 15 μg/kg	11 ± 2[a]	0
	530 MBq/kg ^{177}Lu-IgG1	7 ± 1[a]	0
	530 MBq/kg ^{177}Lu-rituximab	18 ± 4	60
	530 MBq/kg ^{177}Lu-HH1	> 109	0
2	NaCl	6 ± 3	0
	300 MBq/kg ^{177}Lu-rituximab	17 ± 3	0
	410 MBq/kg ^{177}Lu-HH1	> 97	0

[a]Significantly different from ^{177}Lu-HH1 ($p < 0.05$).

doi:10.1371/journal.pone.0128816.t002

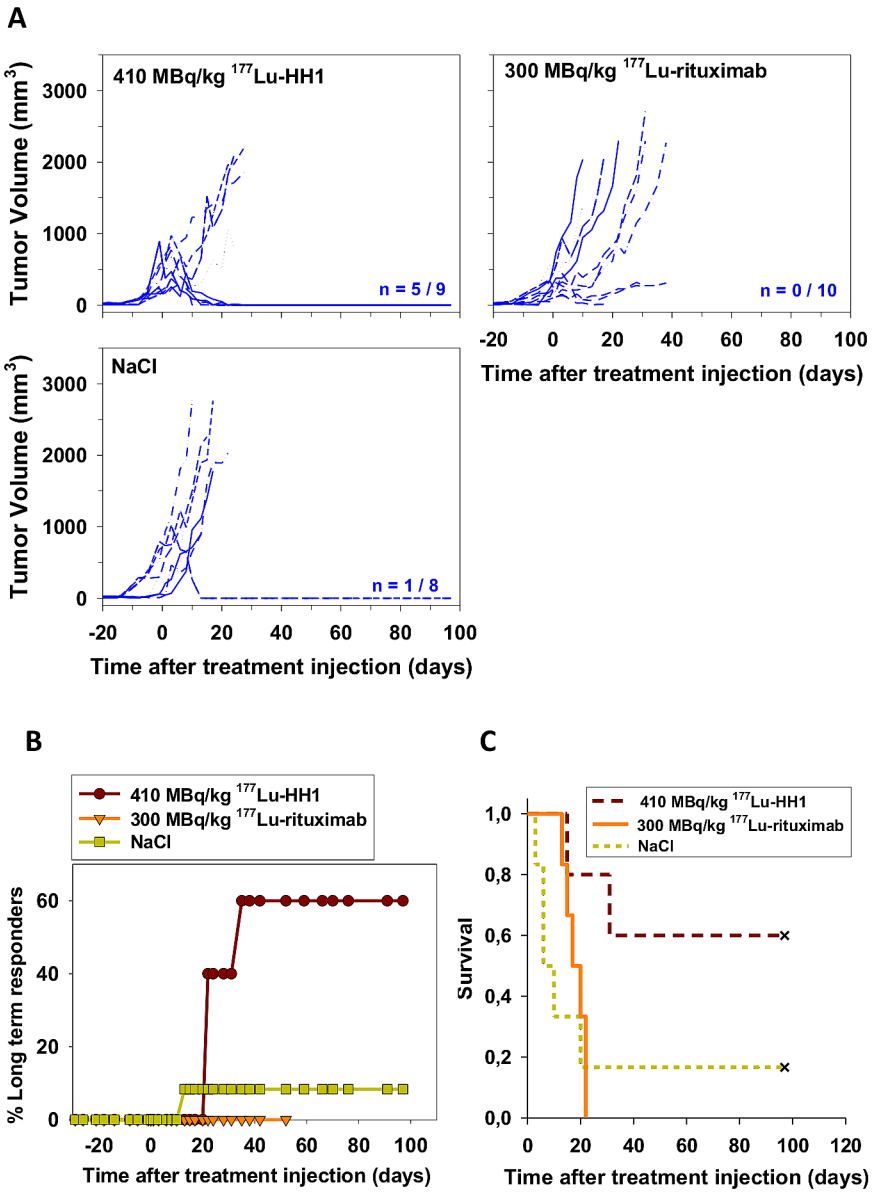

Fig 2. Tumor growth, long term responders and survival of nude mice with Ramos xenografts after treatments with 410 MBq/kg ^{177}Lu-HH1, 300 MBq/kg ^{177}Lu-rituximab and 0.9% NaCl. (A) Individual tumor growth (n = Number of tumors in remission at the end of study/total number of initial tumors) (B) Percentage of long term responders; (C) Kaplan-Meier survival curve. End point: tumor volume ≥ 4 times initial tumor volume. Crosses represent censored animals that were euthanized before reaching 4 times the initial tumor volume. N = 5–6. Multiple comparisons were performed using Holm Sidak method. Significance level: $p < 0.05$.

doi:10.1371/journal.pone.0128816.g002

Similar observations were made for treatments with 800 and 1000 MBq/kg of ^{177}Lu-HH1 [26]. Most of the mice showing severe radiation toxicity symptoms also presented skin hemorrhages (Fig 5B) that started as a skin rash a few days before euthanasia. The histopathology observations were in good agreement with the hematology measurements. For activities of 530 MBq/kg and higher ovaries were affected [26]. Mice euthanized between 11 to 25 days after treatment administration did, however, not show abnormalities in the ovaries, indicating that these lesions take more than 3 weeks to develop.

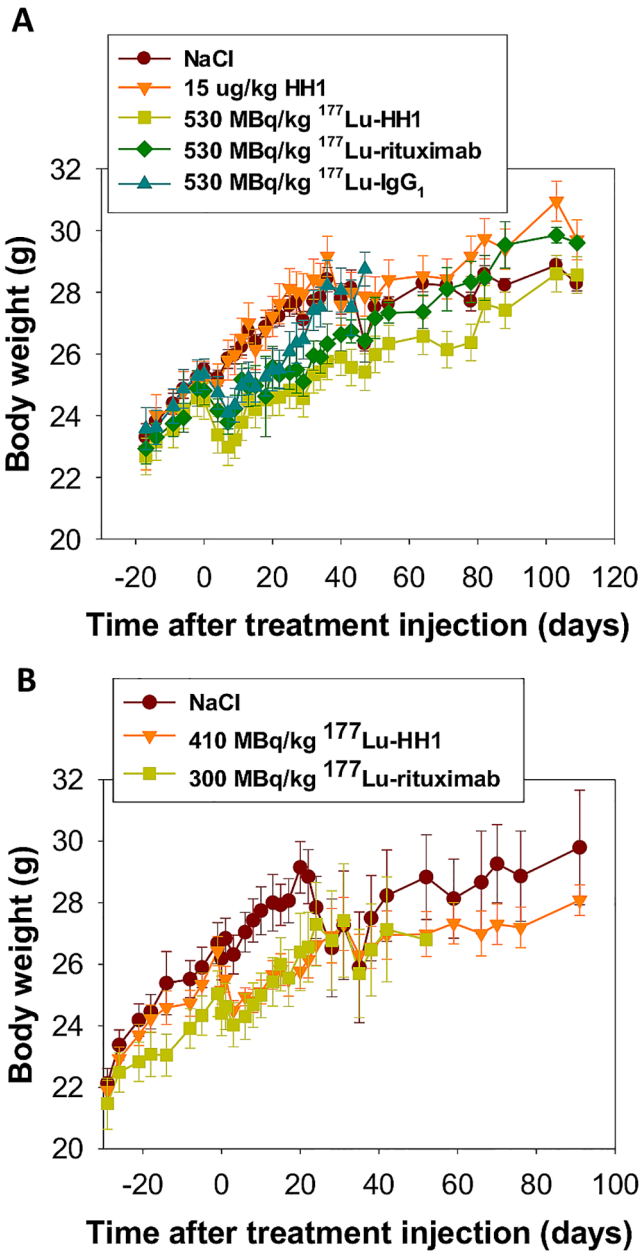

Fig 3. Average Body weight. Average body weight of nude mice with Ramos xenografts treated with 530 MBq/kg ^{177}Lu-HH1, 530 MBq/kg ^{177}Lu-rituximab, 530 MBq/kg ^{177}Lu-IgG$_1$ non-specific isotype control, 15 μg/kg HH1, NaCl 0.9%, 410 MBq/kg ^{177}Lu-HH1 and 300 MBq/kg ^{177}Lu-rituximab.

doi:10.1371/journal.pone.0128816.g003

Biodistribution and dosimetry

Blood clearance was slightly faster for ^{177}Lu-rituximab than for ^{177}Lu-HH1 (Fig 6A), which gave an absorbed dose to blood in mice treated with ^{177}Lu-rituximab around half of that for ^{177}Lu-HH1 (Table 4, Fig 6B). The retention of ^{177}Lu-rituximab in liver, spleen and femur was significantly longer than that of ^{177}Lu-HH1 or ^{177}Lu-IgG$_1$ (Fig 6A and 6B) and consequently absorbed doses to these organs were 2–3 times higher for treatment with ^{177}Lu-rituximab than for ^{177}Lu-HH1. The higher uptake of ^{177}Lu-rituximab in femur (Table 4) probably resulted in a

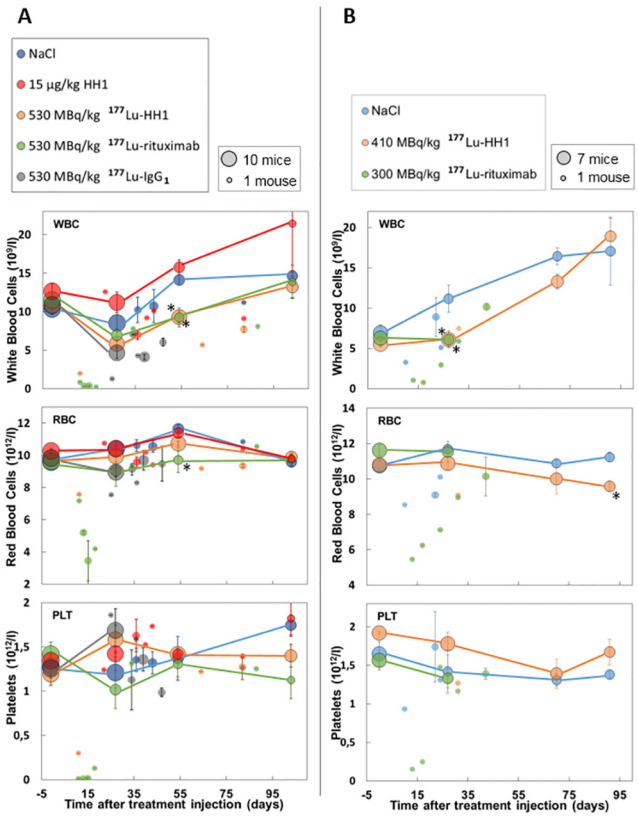

Fig 4. Hematology. Number of white blood cells (WBC), red blood cells (RBC) and platelets (PLT) in mice with Ramos xenografts treated with 530 MBq/kg ^{177}Lu-HH1, 530 MBq/kg ^{177}Lu-rituximab, 530 MBq/kg ^{177}Lu-IgG$_1$ non-specific isotype control, 15 µg/kg HH1, 0.9% NaCl (A) and 410 MBq/kg ^{177}Lu-HH1 and 300 MBq/kg ^{177}Lu-rituximab (B). The area of each circle represents the number of mice used to calculate the average values. Circles with dark rim and connected with lines represent samples taken at fixed time points during the study where all alive mice were sampled. Circles without dark rim and not connected by lines represent blood samples taken before euthanasia, where usually one or two mice were sacrificed. N = 1–10. Error bars = standard error. *: Significantly different from the corresponding 0.9% NaCl (control) group value (One-way ANOVA with Holm Sidak method for multiple comparisons, $p < 0.05$).

doi:10.1371/journal.pone.0128816.g004

higher absorbed dose to red marrow, which is consistent with the higher toxicity and reduced bone marrow cellularity observed in mice treated with ^{177}Lu-rituximab. The uptake in tumor was faster for ^{177}Lu-rituximab, but the retention was shorter (not statistically significant, $p > 0.05$) than for ^{177}Lu-HH1 (Fig 6A). The absorbed doses to tumor were close to 2 Gy for both ^{177}Lu-HH1 and ^{177}Lu-rituximab (Table 4). The uptake and retention of ^{177}Lu-HH1 and ^{177}Lu-IgG$_1$ control were similar for all organs/tissues except for kidneys and tumor (Fig 6A).

SPECT/CT images showed a high and heterogeneous tumor uptake compared with other tissues 48 hours after injection of ^{177}Lu-HH1 (Fig 6C). Uptake in lungs, heart and aorta was high 3 hours after injection and decreased with increasing time, being considerably reduced after 48 hours. Uptake in tumor was low 3 hours after ^{177}Lu-HH1 administration but increased with time and was higher than in other tissues after 48 hours. The difference of tumor uptake measured by SPECT and gamma counter was below 10%, which shows good agreement between measurements performed *in vivo* with SPECT and *ex vivo* by gamma counting.

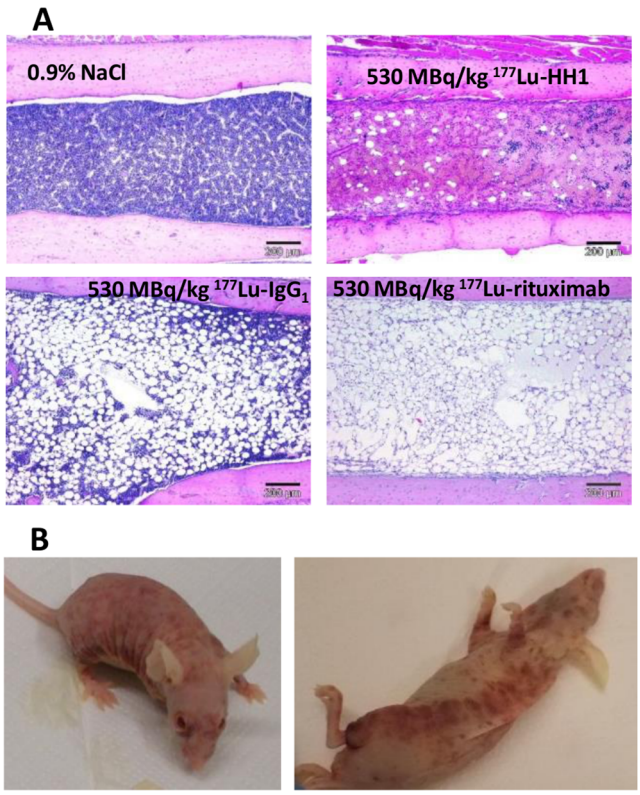

Fig 5. Histopathology. (A) Representative pictures of: a normal bone marrow from a mouse in the NaCl group (euthanized 109 days after treatment), marked reduced cellularity in a mouse treated with 530 MBq/kg ^{177}Lu-HH1 euthanized 11 days after treatment, moderate reduced cellularity in a mouse treated with 530 MBq/kg ^{177}Lu-IgG$_1$ euthanized 25 days after treatment and severe reduced cellularity in a mouse treated with 530 MBq/kg ^{177}Lu-rituximab euthanized 15 days after treatment. (B) Example of a mouse with severe skin hemorrhages 11 days after administration with 530 MBq/kg ^{177}Lu-rituximab. The mouse was sacrificed the day the pictures were taken.

doi:10.1371/journal.pone.0128816.g005

Table 3. Incidence of main histological findings in nude mice with Ramos xenografts treated with 530 MBq/kg ^{177}Lu-HH1, ^{177}Lu-rituxmab and ^{177}Lu-IgG$_1$ non-specific isotype control or 0.9% NaCl.

		Incidence (% (number of mice affected/total number of mice))			
Organ	**Histological finding**	**NaCl**	**530 MBq/kg ^{177}Lu-HH1**	**530 MBq/kg ^{177}Lu-rituximab**	**530 MBq/kg ^{177}Lu-IgG$_1$**
Bone marrow	Reduced cellularity	0 (0/10)	11 (1/9)	60 (6/10)	30 (3/10)
Colon	Lymphoid depletion	0 (0/9)	0 (0/9)	30 (3/10)	30 (3/10)
Ileum	Lymphoid depletion	0 (0/10)	11 (1/9)	10 (1/10)	10 (1/10)
Liver	Extramedullary hematopoiesis	0 (0/10)	0 (0/9)	0 (0/10)	40 (4/10)
	Inflamatory cell infiltration	50 (5/10)	11 (1/9)	10 (1/10)	0 (0/10)
Ovaries	Atretic follicles (present)	0 (0/10)	89 (8/9)	40 (4/10)	100 (8/8)
	Interstitial cell hyperplasia	0 (0/10)	78 (7/9)	40 (4/10)	50 (4/8)
Spleen	Extramedullary hematopoiesis	100 (10/10)	89 (8/9)	40 (4/10)	100 (10/10)
	Lymphoid depletion	10 (1/10)	22 (2/9)	60 (6/10)	80 (8/10)
	Pigmented macrophages	0 (0/10)	11 (1/9)	60 (6/10)	10 (1/10)

doi:10.1371/journal.pone.0128816.t003

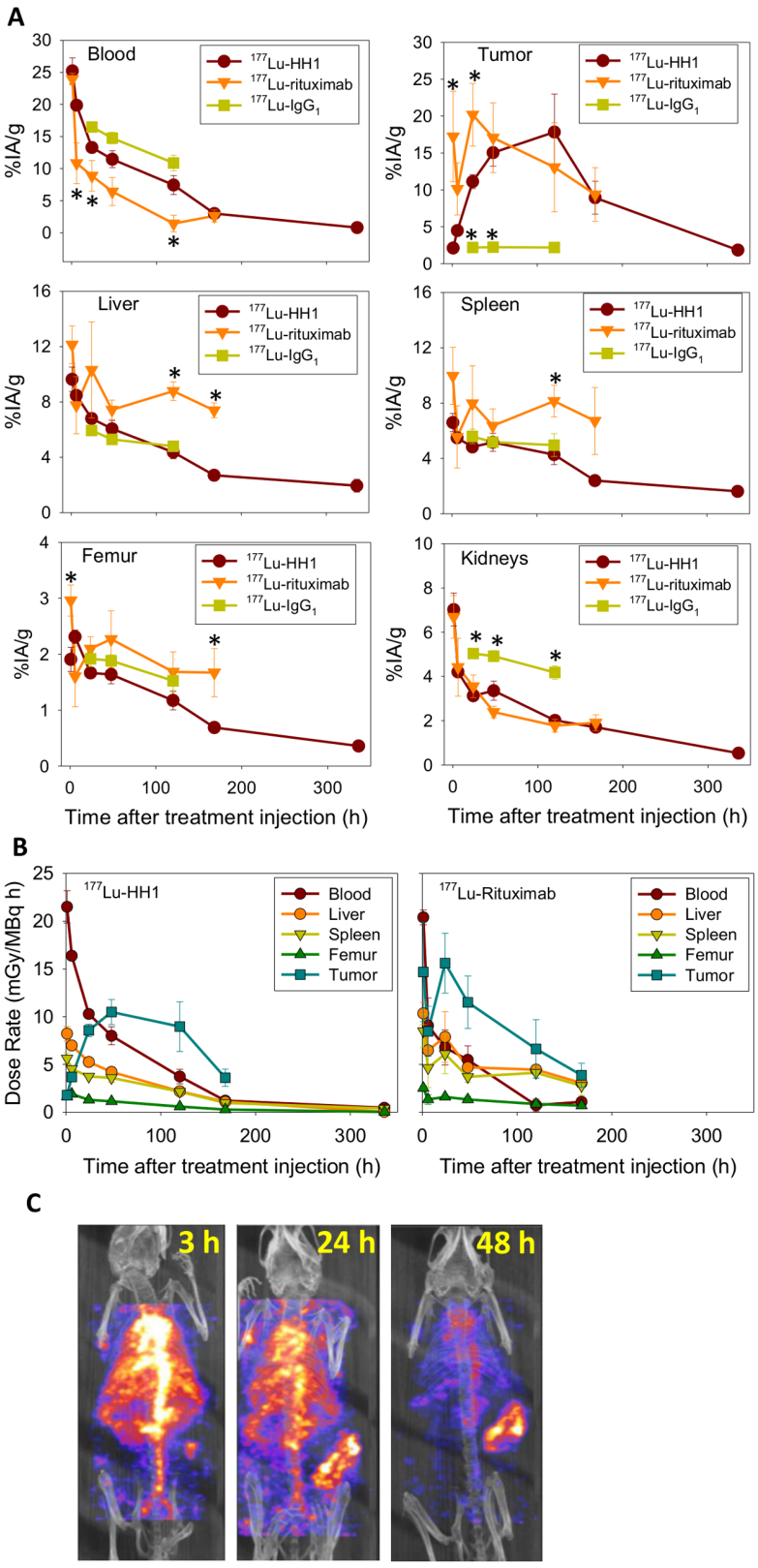

Fig 6. Biodistribution and dosimetry. (A) Uptake of ^{177}Lu-HH1 (N = 6–8), ^{177}Lu-rituximab (N = 4–5), ^{177}Lu-IgG1 control (N = 5) in selected organs/tissues from nude mice with Ramos xenografts in percentage of

injected activity per gram of tissue (%IA/g). Error bars = standard error. *: Significantly different from ^{177}Lu-HH1 (One-way ANOVA with Holm Sidak method for multiple comparisons, $p < 0.05$). (B) Dose rate per MBq of injected activity in selected organs of nude mice with Ramos xenografts treated with ^{177}Lu-HH1 (N = 6–8) and ^{177}Lu-rituximab (N = 4–5). (C) *In vivo* SPECT/CT multiplanar rendered view of a nude mouse with a Ramos xenograft in its right flank injected with 10 MBq of ^{177}Lu-HH1.

doi:10.1371/journal.pone.0128816.g006

Internalization experiments

HH1 was almost completely internalized after 19 hours of incubation at 37°C, while there was no significant internalization after 1 hour incubation at 4°C. Some cells showed HH1 both on the cell surface and inside the cytoplasm while others only showed HH1 inside the cells after 19 hours at 37°C. A small degree of internalization of rituximab was observed after 19 hours of incubation at 37°C, while there was no sign of internalization after 1 hour incubation at 4°C. Fig 7 shows representative images of the cells.

Binding experiments

The number of CD37 antigens per Ramos cell (B_{max}) was half the number of CD20 antigens (Table 5). The dissociation constant (K_d) of HH1 was lower than that of rituximab but the difference was not statistically significant.

Discussion

The majority of the NHL patients nowadays receive anti-CD20 mAbs as first line treatment. The first two RICs on the market, Zevalin and Bexxar, also targeted the same antigen. It has been shown that shaving or downregulation of the CD20 antigen might be a reason for resistance to rituximab [41–43] and it may also be the case for other CD20 based treatments. From a clinical perspective, it is plausible to use another target than CD20 for second line treatment, such as the CD37 antigen. There are currently four drug candidates, in addition to ^{177}Lu-HH1, that target the CD37 antigen: an antibody-based protein [15], an Fc-engineered mAb[17] and two ADCs [19,20]. Given the heterogeneous vascularization and antigen expression normally found in tumors [44,45] it might be useful to develop a treatment that possess cross-fire contribution. We have therefore developed a new RIC (Betalutin) based on ^{177}Lu linked to the anti-CD37 antibody HH1 [24]. The β-emissions of ^{177}Lu have a mean range of 0.67 mm and are able to reach and kill even those cells to which the RIC is not able to bind. A series of pre-clinical studies have shown that ^{177}Lu-HH1 successfully binds to both lymphoma cell lines and biopsies from NHL patients, indicating that targeting of the CD37 antigen with HH1 is clinically

Table 4. Absorbed radiation doses per injected MBq and tumor to normal tissues ratios in selected organs of nude mice with Ramos xenografts administered with ^{177}Lu-HH1 and ^{177}Lu-rituximab.

	Dose (Gy/MBq)		Tumor/Normal Tissue	
Organ/Tissue	^{177}Lu-HH1	^{177}Lu-rituximab	^{177}Lu-HH1	^{177}Lu-rituximab
Blood	1,26 ± 0,06	0,72 ± 0,1	1,7 ± 0,2	2,5 ± 0,5
Liver	0,71 ± 0,05	1,4 ± 0,1	2,9 ± 0,4	1,3 ± 0,2
Spleen	0,54 ± 0,01	1,3 ± 0,3	3,8 ± 0,5	1,3 ± 0,26
Kidney	0,36 ± 0,01	0,36 ± 0,03	5,8 ± 0,8	5,0 ±- 0,9
Femur	0,093 ± 0,001	0,15 ± 0,02	22,3 ±- 3,0	12,0 ±- 2,4
Tumor	2,1 ± 0,3	1,8 ± 0,3	——-	——-

doi:10.1371/journal.pone.0128816.t004

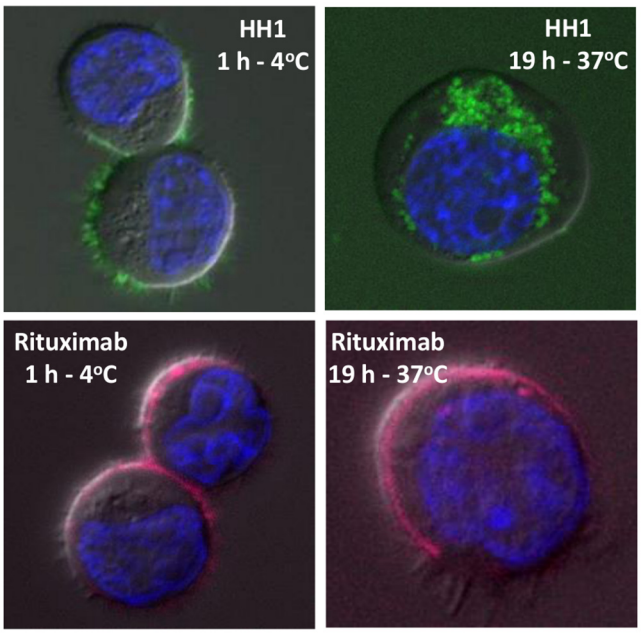

Fig 7. Internalization. Representative images of internalization of HH1 and Rituximab in Ramos cells after incubation with 10 μg/ml of HH1 or 20 μg/ml rituximab at 4°C or 37°C for 1 hour or 19 hours, respectively. HH1-DOTA bound to Alexa Fluor 488 is shown in green, Rituximab bound to Alexa Fluor 647 is shown in magenta and Hoechst 33342 bound to DNA in the cell nucleus is shown in blue. 20 to 40 cells were scanned for each treatment.

doi:10.1371/journal.pone.0128816.g007

relevant [7]. Furthermore, the biodistribution of ^{177}Lu-HH1 was found to be relevant for the treatment of NHL in SCID mice i.v. injected with Daudi lymphoma cells and in nude mice with Daudi [28] and Ramos subcutaneous xenografts as shown in Fig 6. In addition, *in vivo* experiments in SCID mice showed that ^{177}Lu-HH1 had a strong therapeutic effect, increasing the survival of treated mice compared with mice treated with unlabeled HH1 and NaCl [7]. The current study shows that ^{177}Lu-HH1 has strong antitumor activity and lower toxicity compared with ^{177}Lu-rituximab in nude mice with subcutaneous Ramos xenografts. Even though Ramos cells had a higher expression of CD20 than CD37, the absorbed doses to tumor for ^{177}Lu-HH1 and ^{177}Lu-rituximab were similar, which might be related to the higher internalization of the CD37-HH1 complex than of the CD20-rituximab, as observed *in vitro*. It has been reported previously that human cells are highly heterogeneous in their ability to internalize CD20 when bound to mAbs [46], ranging from lack of internalization [8,47–49] to high internalization [50–53]. The higher myelotoxicity of ^{177}Lu-rituximab than of ^{177}Lu-HH1 might be explained by a higher uptake and retention of ^{177}Lu-rituximab in the bone marrow as indicated by the higher uptake and retention in the femur, spleen and liver (Fig 6). The higher uptake and retention of

Table 5. Maximum number of CD37 and CD20 antigens (B_{max}) and equilibrium dissociation constant (K_d) of ^{177}Lu-HH1 and ^{125}I-rituximab in Ramos cells.

Antibody (antigen)	K_d (nM)	B_{max} (antigens/cell)
HH1 (CD37)	1.6 ± 1	128000 ± 40000
Rituximab (CD20)	2.4 ± 1	279000 ± 51000

Results presented as average ± standard deviation. N = 2 for rituximab, N = 3 for HH1.

doi:10.1371/journal.pone.0128816.t005

^{177}Lu-rituximab in femur and spleen was not correlated with the high uptake and retention in the blood, but for myelotoxicity the cumulated activity in the bone marrow is more relevant than the cumulated activity in the blood. The uptake and retention in bone marrow is probably estimated better by the biodistribution data for femur than for blood. Another mechanism that might have played a role for the difference in toxicity and therapeutic effect of ^{177}Lu-rituximab and ^{177}Lu-HH1 is the difference in shaving of the antigen-antibody complex for CD20:rituximab and CD37:HH1 [52,54]. Treatment with ^{177}Lu-HH1 had a strong anti-tumor effect in the nude mice even though the tumor uptake was inhomogeneous as shown in the SPECT/CT images. This result implies that cross-fire effect might play an important role in the therapeutic effect of ^{177}Lu-HH1.

The toxicity data presented indicates that the dose-limiting organ is the bone marrow, which is in agreement with previous studies in mice and humans showing that the most common and dose-limiting side effect of RIT is bone marrow toxicity [26,55]. The maximum tolerated activities (MTA) in nude mice can be assumed to be 550 MBq/kg = 1667 MBq/m^2 for ^{177}Lu-HH1 and 400 MBq/kg = 1212 MBq/m^2 for ^{177}Lu-rituximab (allometric equivalence performed on the basis of Body Surface Area [56–60]). These values are in relatively good agreement with the clinical MTA of ^{177}Lu-rituximab found by Forrer *et al.* of 1665 MBq/m^2 in humans [61].

CD37 internalizes, and has modest shedding in transformed B-cells expressing this antigen [8,47]. The early studies with ^{131}I-MB-1 have probably underestimated the potential of CD37 as target for RIT due to the use of a "non-residualizing" radiolabel. We have previously shown that the use of the "residualizing" radiolabel ^{177}Lu chelated via a DOTA linker to HH1 increased the uptake of the RIC in tumor compared to the RIC ^{125}I-HH1 up to 20 times [23]. This could at least partly be related to the accumulation of "residualizing" ^{177}Lu inside the cells due to the internalizing nature of CD37 [23].

In summary, ^{177}Lu-HH1 is a promising RIC as treatment against CD37-expressing NHL and the antitumor activity and the toxicity profile found in the preclinical studies supports further clinical investigation.

Conclusion

This paper has shown, through comparisons of treatments of ^{177}Lu-HH1, ^{177}Lu-rituximab and non-specific ^{177}Lu-IgG$_1$ isotype control in nude mice with subcutaneous Ramos lymphoma xenografts, that ^{177}Lu-HH1 has very promising properties as a treatment of NHL. ^{177}Lu-HH1 considerably delayed tumor growth, increased the number of complete remissions and increased the survival of nude mice. In addition, ^{177}Lu-HH1 was less toxic than ^{177}Lu-rituximab. Based on these findings we conclude that ^{177}Lu-HH1 is a promising agent for treatment of NHL and clinical evaluation is recommended.

Supporting Information

S1 File. Preliminary Experiments. Therapy results from the preliminary experiments that assisted in the design of the experiments presented in the paper.
(PDF)

Acknowledgments

The technical contributions of Ellena Riccardi from Accelera are highly appreciated.

Author Contributions

Conceived and designed the experiments: AHVRL RHL SP DD AP JPP JD. Performed the experiments: AHVRL SP KGF DD AP. Analyzed the data: AHVRL SP KGF RHL DD AP JPP JD.

Contributed reagents/materials/analysis tools: AHVRL SP KGF RHL DD AP JPP JD. Wrote the paper: AHVRL RHL SP DD AP JPP JD.

References

1. Flinn IW, van der Jagt R, Kahl BS, Wood P, Hawkins TE, MacDonald D, et al. (2014) Randomized trial of bendamustine-rituximab or R-CHOP/R-CVP in first-line treatment of indolent NHL or MCL: the BRIGHT study. Blood 123: 2944–2952. doi: 10.1182/blood-2013-11-531327 PMID: 24591201
2. Kaminski MS, Estes J, Zasadny KR, Francis IR, Ross CW, Tuck M, et al. (2000) Radioimmunotherapy with iodine (131)I tositumomab for relapsed or refractory B-cell non-Hodgkin lymphoma: updated results and long-term follow-up of the University of Michigan experience. Blood 96: 1259–1266. PMID: 10942366
3. Kaminski MS, Tuck M, Estes J, Kolstad A, Ross CW, Zasadny K, et al. (2005) 131I-tositumomab therapy as initial treatment for follicular lymphoma. N Engl J Med 352: 441–449. PMID: 15689582
4. Witzig TE, Flinn IW, Gordon LI, Emmanouilides C, Czuczman MS, Saleh MN, et al. (2002) Treatment with ibritumomab tiuxetan radioimmunotherapy in patients with rituximab-refractory follicular non-Hodgkin's lymphoma. J Clin Oncol 20: 3262–3269. PMID: 12149300
5. Witzig TE, Gordon LI, Cabanillas F, Czuczman MS, Emmanouilides C, Joyce R, et al. (2002) Randomized controlled trial of yttrium-90-labeled ibritumomab tiuxetan radioimmunotherapy versus rituximab immunotherapy for patients with relapsed or refractory low-grade, follicular, or transformed B-cell non-Hodgkin's lymphoma. J Clin Oncol 20: 2453–2463. PMID: 12011122
6. Moldenhauer G (2000) CD37. J Biol Regul Homeost Agents 14: 281–283. PMID: 11215818
7. Dahle J, Repetto-Llamazares AH, Mollatt CS, Melhus KB, Bruland OS, Kolstad A, et al. (2013) Evaluating antigen targeting and anti-tumor activity of a new anti-CD37 radioimmunoconjugate against non-Hodgkin's lymphoma. Anticancer Res 33: 85–95. PMID: 23267131
8. Press OW, Howell-Clark J, Anderson S, Bernstein I (1994) Retention of B-cell-specific monoclonal antibodies by human lymphoma cells. Blood 83: 1390–1397. PMID: 8118040
9. Brown RS, Kaminski MS, Fisher SJ, Chang AE, Wahl RL (1997) Intratumoral microdistribution of [131I] MB-1 in patients with B-cell lymphoma following radioimmunotherapy. Nucl Med Biol 24: 657–663. PMID: 9352537
10. Buchsbaum DJ, Wahl RL, Normolle DP, Kaminski MS (1992) Therapy with unlabeled and 131I-labeled pan-B-cell monoclonal antibodies in nude mice bearing Raji Burkitt's lymphoma xenografts. Cancer Res 52: 6476–6481. PMID: 1423295
11. Eary JF, Press OW, Badger CC, Durack LD, Richter KY, Addison SJ, et al. (1990) Imaging and treatment of B-cell lymphoma. J Nucl Med 31: 1257–1268. PMID: 2384792
12. Kaminski MS, Fig LM, Zasadny KR, Koral KF, DelRosario RB, Francis IR, et al. (1992) Imaging, dosimetry, and radioimmunotherapy with iodine 131-labeled anti-CD37 antibody in B-cell lymphoma. J Clin Oncol 10: 1696–1711. PMID: 1403053
13. Press OW, Eary JF, Badger CC, Martin PJ, Appelbaum FR, Levy R, et al. (1989) Treatment of refractory non-Hodgkin's lymphoma with radiolabeled MB-1 (anti-CD37) antibody. J Clin Oncol 7: 1027–1038. PMID: 2666588
14. Press OW, Eary JF, Appelbaum FR, Martin PJ, Badger CC, Nelp WB, et al. (1993) Radiolabeled-antibody therapy of B-cell lymphoma with autologous bone marrow support. N Engl J Med 329: 1219–1224. PMID: 7692295
15. Gopal AK, Tarantolo SR, Bellam N, Green DJ, Griffin M, Feldman T, et al. (2014) Phase 1b study of otlertuzumab (TRU-016), an anti-CD37 monospecific ADAPTIR therapeutic protein, in combination with rituximab and bendamustine in relapsed indolent lymphoma patients. Invest New Drugs.
16. Robak T, Hellman A, Kloczko J, Loscertales J, Lech-Maranda E, Pagel J, et al. (2013) Phase 2 Study of Otlertuzumab (TRU-016), an anti-CD37 ADAPTIR protein, in combination with bendamustine vs bendamustine alone in patients with relapsed Chronic Lymphocytic Leukemia (CLL). 55th American Society of Hematology Annual Meeting and Exposition.
17. Heider KH, Kiefer K, Zenz T, Volden M, Stilgenbauer S, Ostermann E, et al. (2011) A novel Fc-engineered monoclonal antibody to CD37 with enhanced ADCC and high proapoptotic activity for treatment of B-cell malignancies. Blood 118: 4159–4168. doi: 10.1182/blood-2011-04-351932 PMID: 21795744
18. BI 836826 Dose Escalation in Patients With Relapsed or Refractory Non-Hodgkin Lymphoma (NHL). Available: http://clinicaltrials.gov/show/NCT01403948. Accessed 2014 Oct 10.
19. Beckwith KA, Frissora FW, Stefanovski MR, Towns WH, Cheney C, Mo X, et al. (2014) The CD37-targeted antibody-drug conjugate IMGN529 is highly active against human CLL and in a novel CD37

transgenic murine leukemia model. Leukemia 28: 1501–1510. doi: 10.1038/leu.2014.32 PMID: 24445867

20. Deckert J, Park PU, Chicklas S, Yi Y, Li M, Lai KC, et al. (2013) A novel anti-CD37 antibody-drug conjugate with multiple anti-tumor mechanisms for the treatment of B-cell malignancies. Blood 122: 3500–3510. doi: 10.1182/blood-2013-05-505685 PMID: 24002446
21. Ansell SM (2014) Brentuximab vedotin. Blood.
22. Oostra DR, Macrae ER (2014) Role of trastuzumab emtansine in the treatment of HER2-positive breast cancer. Breast Cancer (Dove Med Press) 6: 103–113. doi: 10.2147/BCTT.S67297 PMID: 25114588
23. Repetto-Llamazares A, Abbas N, Bruland OS, Dahle J, Larsen RH (2014) Advantage of Lutetium-177 versus Radioiodine Immunoconjugate in Targeted Radionuclide Therapy of B-cell Tumors. Anticancer Res 34: 3263–3269. PMID: 24982330
24. Smeland E, Funderud S, Ruud E, Kiil BH, Godal T (1985) Characterization of two murine monoclonal antibodies reactive with human B cells. Their use in a high-yield, high-purity method for isolation of B cells and utilization of such cells in an assay for B-cell stimulating factor. Scand J Immunol 21: 205–214. PMID: 3887557
25. Fulop GM, Phillips RA (1990) The scid mutation in mice causes a general defect in DNA repair. Nature 347: 479–482. PMID: 2215662
26. Repetto-Llamazares AH, Larsen RH, Giusti AM, Riccardi E, Bruland OS, Selbo PK, et al. (2014) 177Lu-DOTA-HH1, a Novel Anti-CD37 Radio-Immunoconjugate: A Study of Toxicity in Nude Mice. PLoS One 9: e103070. doi: 10.1371/journal.pone.0103070 PMID: 25068508
27. Lindmo T, Boven E, Cuttitta F, Fedorko J, Bunn PA Jr (1984) Determination of the immunoreactive fraction of radiolabeled monoclonal antibodies by linear extrapolation to binding at infinite antigen excess. J Immunol Methods 72: 77–89. PMID: 6086763
28. Repetto-Llamazares AH, Larsen RH, Mollatt C, Lassmann M, Dahle J (2013) Biodistribution and dosimetry of (177)Lu-tetulomab, a new radioimmunoconjugate for treatment of non-Hodgkin lymphoma. Curr Radiopharm 6: 20–27. PMID: 23256748
29. National Nuclear Data Center, ENSDF Decay Data in the MIRD (Medical Internal Radiation Dose) Format for 177Lu. Available: http://www.nndc.bnl.gov/useroutput/177lu_mird.html. Accessed 2012 Oct 16.
30. Miller WH, Hartmann-Siantar C, Fisher D, Descalle MA, Daly T, Lehmann J, et al. (2005) Evaluation of beta-absorbed fractions in a mouse model for 90Y, 188Re, 166Ho, 149Pm, 64Cu, and 177Lu radionuclides. Cancer Biother Radiopharm 20: 436–449. PMID: 16114992
31. Press OW, Corcoran M, Subbiah K, Hamlin DK, Wilbur DS, Johnson T, et al. (2001) A comparative evaluation of conventional and pretargeted radioimmunotherapy of CD20-expressing lymphoma xenografts. Blood 98: 2535–2543. PMID: 11588052
32. Silobrcic V, Zietman AL, Ramsay JR, Suit HD, Sedlacek RS (1990) Residual immunity of athymic NCr/Sed nude mice and the xenotransplantation of human tumors. Int J Cancer 45: 325–333. PMID: 2406204
33. Cavacini LA, Giles-Komar J, Kennel M, Quinn A (1992) Effect of immunosuppressive therapy on cytolytic activity of immunodeficient mice: implications for xenogeneic transplantation. Cell Immunol 144: 296–310. PMID: 1394445
34. Naumovski L, Ramos J, Sirisawad M, Chen J, Thiemann P, Lecane P, et al. (2005) Sapphyrins induce apoptosis in hematopoietic tumor-derived cell lines and show in vivo antitumor activity. Mol Cancer Ther 4: 968–976. PMID: 15956254
35. Manders JM, Postema EJ, Corstens FH, Boerman OC (2002) Enhancing tumor implantation and growth rate of Ramos B-cell lymphoma in nude mice. Comp Med 52: 36–38. PMID: 11902151
36. Nauta MM, Boven E, Schluper HM, Erkelens CA, Pinedo HM (1986) Enhanced transplantability of human ovarian cancer lines in cyclophosphamide-pretreated nude mice. Br J Cancer 54: 331–335. PMID: 3017398
37. Postema EJ, Frielink C, Oyen WJ, Raemaekers JM, Goldenberg DM, Corstens FH, et al. (2003) Biodistribution of 131I-, 186Re-, 177Lu-, and 88Y-labeled hLL2 (Epratuzumab) in nude mice with CD22-positive lymphoma. Cancer Biother Radiopharm 18: 525–533. PMID: 14503946
38. Park SI, Shenoi J, Pagel JM, Hamlin DK, Wilbur DS, Orgun N, et al. (2010) Conventional and pretargeted radioimmunotherapy using bismuth-213 to target and treat non-Hodgkin lymphomas expressing CD20: a preclinical model toward optimal consolidation therapy to eradicate minimal residual disease. Blood 116: 4231–4239. doi: 10.1182/blood-2010-05-282327 PMID: 20702781
39. Mattes MJ, Sharkey RM, Karacay H, Czuczman MS, Goldenberg DM (2008) Therapy of advanced B-lymphoma xenografts with a combination of 90Y-anti-CD22 IgG (epratuzumab) and unlabeled anti-CD20 IgG (veltuzumab). Clin Cancer Res 14: 6154–6160. doi: 10.1158/1078-0432.CCR-08-0404 PMID: 18829494

40. Martin SM, Churchill E, McKnight H, Mahaffey CM, Ma Y, O'Donnell RT, et al. (2011) The HB22.7 Anti-CD22 monoclonal antibody enhances bortezomib-mediated lymphomacidal activity in a sequence dependent manner. J Hematol Oncol 4: 49. doi: 10.1186/1756-8722-4-49 PMID: 22128838

41. Beers SA, French RR, Chan HT, Lim SH, Jarrett TC, Vidal RM, et al. (2010) Antigenic modulation limits the efficacy of anti-CD20 antibodies: implications for antibody selection. Blood 115: 5191–5201. doi: 10.1182/blood-2010-01-263533 PMID: 20223920

42. Davis TA, Grillo-Lopez AJ, White CA, McLaughlin P, Czuczman MS, Link BK, et al. (2000) Rituximab anti-CD20 monoclonal antibody therapy in non-Hodgkin's lymphoma: safety and efficacy of re-treatment. J Clin Oncol 18: 3135–3143. PMID: 10963642

43. Pham T, Mero P, Booth JW (2011) Dynamics of macrophage trogocytosis of rituximab-coated B cells. PLoS One 6: e14498. doi: 10.1371/journal.pone.0014498 PMID: 21264210

44. Graff BA, Kvinnsland Y, Skretting A, Rofstad EK (2003) Intratumour heterogeneity in the uptake of macromolecular therapeutic agents in human melanoma xenografts. Br J Cancer 88: 291–297. PMID: 12610516

45. Kvinnsland Y, Stokke T, Aurlien E (2001) Radioimmunotherapy with alpha-particle emitters: microdosimetry of cells with a heterogeneous antigen expression and with various diameters of cells and nuclei. Radiat Res 155: 288–296. PMID: 11175663

46. Beers SA, Chan CH, French RR, Cragg MS, Glennie MJ (2010) CD20 as a target for therapeutic type I and II monoclonal antibodies. Semin Hematol 47: 107–114. doi: 10.1053/j.seminhematol.2010.01.001 PMID: 20350657

47. Press OW, Farr AG, Borroz KI, Anderson SK, Martin PJ (1989) Endocytosis and degradation of monoclonal antibodies targeting human B-cell malignancies. Cancer Res 49: 4906–4912. PMID: 2667754

48. Vervoordeldonk SF, Balkenende AY, van den Berg H, von dem Borne AE, van der Schoot CE, Van Leeuwen EF, et al. (1996) Degradation of radioiodinated B cell monoclonal antibodies: inhibition via a FCgamma-receptor-II-mediated mechanism and by drugs. Cancer Immunol Immunother 42: 24–30. PMID: 8625363

49. Braslawsky GR, Kadow K, Knipe J, McGoff K, Edson M, Kaneko T, et al. (1991) Adriamycin(hydrazone)-antibody conjugates require internalization and intracellular acid hydrolysis for antitumor activity. Cancer Immunol Immunother 33: 367–374. PMID: 1878890

50. Vaughan AT, Iriyama C, Beers SA, Chan CH, Lim SH, Williams EL, et al. (2014) Inhibitory FcgammaRIIb (CD32b) becomes activated by therapeutic mAb in both cis and trans and drives internalization according to antibody specificity. Blood 123: 669–677. doi: 10.1182/blood-2013-04-490821 PMID: 24227819

51. Michel RB, Mattes MJ (2002) Intracellular accumulation of the anti-CD20 antibody 1F5 in B-lymphoma cells. Clin Cancer Res 8: 2701–2713. PMID: 12171904

52. Beum PV, Peek EM, Lindorfer MA, Beurskens FJ, Engelberts PJ, Parren PW, et al. (2011) Loss of CD20 and bound CD20 antibody from opsonized B cells occurs more rapidly because of trogocytosis mediated by Fc receptor-expressing effector cells than direct internalization by the B cells. J Immunol 187: 3438–3447. doi: 10.4049/jimmunol.1101189 PMID: 21841127

53. Sieber T, Schoeler D, Ringel F, Pascu M, Schriever F (2003) Selective internalization of monoclonal antibodies by B-cell chronic lymphocytic leukaemia cells. Br J Haematol 121: 458–461. PMID: 12716368

54. Boross P, Leusen JH (2012) Mechanisms of action of CD20 antibodies. Am J Cancer Res 2: 676–690. PMID: 23226614

55. Sharkey RM, Blumenthal RD, Hansen HJ, Goldenberg DM (1990) Biological considerations for radioimmunotherapy. Cancer Res 50: 964s–969s. PMID: 2297750

56. Freireich EJ, Gehan EA, Rall DP, Schmidt LH, Skipper HE (1966) Quantitative comparison of toxicity of anticancer agents in mouse, rat, hamster, dog, monkey, and man. Cancer Chemother Rep 50: 219–244. PMID: 4957125

57. Goldsmith MA, Slavik M, Carter SK (1975) Quantitative prediction of drug toxicity in humans from toxicology in small and large animals. Cancer Res 35: 1354–1364. PMID: 804350

58. Olson H, Betton G, Robinson D, Thomas K, Monro A, Kolaja G, at al. (2000) Concordance of the toxicity of pharmaceuticals in humans and in animals. Regul Toxicol Pharmacol 32: 56–67. PMID: 11029269

59. Greaves P, Williams A, Eve M (2004) First dose of potential new medicines to humans: how animals help. Nat Rev Drug Discov 3: 226–236. PMID: 15031736

60. Reagan-Shaw S, Nihal M, Ahmad N (2008) Dose translation from animal to human studies revisited. FASEB J 22: 659–661. PMID: 17942826

61. Forrer F, Oechslin-Oberholzer C, Campana B, Herrmann R, Maecke HR, Mueller-Brand J, et al. (2013) Radioimmunotherapy with 177Lu-DOTA-rituximab: final results of a phase I/II Study in 31 patients with relapsing follicular, mantle cell, and other indolent B-cell lymphomas. J Nucl Med 54: 1045–1052. doi: 10.2967/jnumed.112.115170 PMID: 23572496